

The FS Model

The intrinsic dynamics of the FS cells were given by the conductance-based model for neocortical FS interneurons by Erisir et al. (1999) as modified in Jolivet et al. (2004) and Lewis and Rinzel (2004):

$$C_m \frac{dV}{dt} = -I_{ionic}(V, m, h, n, p) + I_{applied}$$

$$\frac{dy}{dt} = \frac{y_{\infty}(V) - y}{\tau_y(V)}, \quad y = m, h, n, p$$

where V is the membrane potential of the cell, m , h , n and p are the gating variables, C_m is the membrane capacitance, and $I_{applied}$ is the current applied.

$$I_{ionic}(V, m, h, n, p) = I_{Na} + I_{Kv3} + I_{Kv1} + I_{leak}$$

$$I_{Na} = g_{Na} m^3 h (V - V_{Na})$$

$$I_K = (g_{Kv3} p^2 + g_{Kv1} n^4) (V - V_K)$$

$$I_{leak} = g_{leak} (V - V_{leak})$$

where the reversal potentials are $V_{Na}=74$ mV, $V_K=-90$ mV, $V_{leak}=-70$ mV, the maximal ionic conductances are $g_{Na}=4500$ nS (112.5 mS/cm²), $g_{Kv3}=9000$ nS (225.0 mS/cm²), $g_{Kv1}=9$ nS (0.225 mS/cm²), $g_{leak}=10$ nS (0.25 mS/cm²), and $C_m=40$ pF (1 μF/cm²). The surface area of the cell is 0.00004 cm².

The equation for the gating variables $y = m, h, n$ and p can be written as

$$\frac{dy}{dt} = \alpha_y(V)(1 - y) - \beta_y(V)y$$

$$y_{\infty}(V) = \frac{\alpha_y(V)}{\alpha_y(V) + \beta_y(V)}$$

$$\tau_y(V) = \frac{1}{\alpha_y(V) + \beta_y(V)}$$

where

$$\alpha_m(V) = \frac{40 (V - 75.5)}{1 - \exp(-(V - 75.5)/13.5)}$$

$$\beta_m(V) = \frac{1.2262}{\exp(V/42.248)}$$

$$\alpha_h(V) = \frac{0.0035}{\exp(V/24.186)}$$

$$\beta_h(V) = \frac{0.017 (51.25 + V)}{1 - \exp(-(51.25 + V)/5.2)}$$

$$\alpha_p(V) = \frac{(V - 95)}{1 - \exp(-(V - 95)/11.8)}$$

$$\beta_p(V) = \frac{0.025}{\exp(V/22.222)}$$

$$\alpha_n(V) = \frac{0.014 (V + 44)}{1 - \exp(-(V + 44)/2.3)}$$

$$\beta_n(V) = \frac{0.0043}{\exp((V + 44.0)/34.0)} .$$

The model description and the parameters are the same as those in the original Erisir et al. model except that the leakage conductance, g_{leak} , was divided by 5 to better match the membrane time constants of cortical FS cells (Beierlein et al., 2003), and the membrane surface area was increased by a factor of 5 to better match the experimentally measured input resistance of FS cells. Note that a corrigendum for Erisir et al. 1999 was published [in *J. Neurophysiol.* 84, p.11 \(2000\).](#)

Supplementary Figure S1. The magnitude of the jitter as a function of the mean period. Single FS and LTS cells were made to fire repetitively by injection of current ramps and current steps (see methods). Distributions of inter-spike intervals (ISIs) were compiled, and the mean ISI (mean period, T) and the corresponding standard deviation in ISI (σ) were computed. σ was plotted in relation to T , and these data were then fitted to second order polynomials. FS cells, ramp responses: $\sigma = (0.051T)^2 - 0.049T + 0.51$ (n=16); LTS cells, ramp responses: $\sigma = (0.040T)^2 - 0.048T + 1.2$ (n=11); FS cells, step responses: $\sigma = (0.027T)^2 - 0.024T + 0.022$ (n=23). LTS cells, step responses: $\sigma = -(0.015T)^2 + 0.066T + 0.11$ (n=11). For responses to current ramps, data were divided into time windows that included 20 spikes over which the frequency was approximately stationary. For responses evoked by the current steps, only spikes in the final 900 ms of each trial were used.

Supplementary Figure S2. Phase-response curves (PRCs) for a real FS cell firing at **(A)** 53 Hz and **(B)** 32 Hz. Top traces show single periods of the membrane potentials (V_θ), and middle traces show the corresponding phase-response curves ($Z(t)$ in units of pA^{-1}). Multiple cycles of V_θ are shown in grey and the cycle with the median period is shown in black. Experimental data points on the PRC are shown in grey and the fitted curve is shown in black. Bottom traces show the corresponding G-functions $G(\phi)$ for a pair of electrically coupled cells (in units of nS^{-1}). The height of $G(\phi)$ is proportional to the coupling strength g_{coup} . The zeros of $G(\phi)$ indicate the phase of the phase-locked states. When the slope of $G(\phi)$ is negative at the zero, the corresponding phase-locked state is stable. Conversely when the slope is positive, the phase locked state is unstable. The G-functions for the “real” FS cell pair at both 53 Hz and 32 Hz indicate that only synchrony ($\phi=0,2\pi$) is stable.

Supplementary Figure S3. Phase-response curves (PRCs) for different real FS cells firing at various frequencies. The first column shows single periods of the membrane potentials (V_θ), and the middle column shows the corresponding phase-response curves ($Z(t)$ in units of pA^{-1}). Multiple cycles of V_θ are shown in grey, and the cycle with the median period is shown in black. Experimental data points on the PRC are shown in grey and the fitted curve is shown in black. The last column shows the corresponding G-functions $G(\phi)$ for a pair of electrically coupled cells (in units of nS^{-1}). All G-functions for the FS cells indicate that only synchrony is stable. Data for FS cells (iii)-(ix) are shown; data for FS cells (i) and (ii) are shown in Figure 2 and Supplementary Figure S2.

Supplementary Figure S4. Phase-response curves (PRCs) for different real LTS cells firing at various frequencies. The first column shows single periods of the membrane potentials (V_θ), and the middle column shows the corresponding phase-response curves ($Z(t)$ in units of pA^{-1}). Multiple cycles of V_θ are shown in grey and the cycle with the median period is shown in black. Experimental data points on the PRC are shown in grey and the fitted curve is shown in black. The last column shows the corresponding G-functions $G(\phi)$ for a pair of electrically coupled cells (in units of nS^{-1}). All G-functions for the LTS cells indicate that only synchrony is stable.

Supplementary Figure S5. Population data for pairs of FS and LTS cells obtained with simultaneous current steps. CC_0 (top), R^2 (middle) and average phase Φ (bottom) are plotted against frequency for single trials. Each symbol represents a different pair with the coupling strength (c_s) indicated in the legend and is maintained for all plots within a column. Open symbols are for pairs with $c_s < 0.1$; closed symbols are for pairs with $c_s > 0.1$. The dashed curves in the plots of CC_0 and R^2 vs frequency are p -value level curves as computed with the random jitter model (black dashed line $p=0.5$; red dashed line $p=0.005$). The data suggests an increase in synchrony with increases in coupling strength, but no conclusive dependence of synchrony on frequency.

Supplementary Figure S6. The phase-difference of phase-locked states *vs* the normalized difference in intrinsic frequency as predicted by the theory of weakly coupled oscillators and the experimentally determined PRC-functions in Fig.2.

Supplementary Figure S7. Normalized peak of correlation function at $\phi=0$ ($\rho(0)$) vs firing frequency. Correlation functions were computed using the 11 experimentally determined G-functions for FS cells and the method described in Pfeuty et al. (2005). All peaks of the correlation functions are at $\phi=0$. Two different models for the intrinsic noise of the cells were used. (i) Intrinsic cellular noise was described by the statistics of our jitter measurements from individual cells in which the coefficient of variation of the jitter decreased with frequency (see supplementary Fig.1). Data points are indicated by open circle; linear fit of data is indicated by solid line (slope=0.0136, $r=0.126$). There is a clear increase of peak correlation with frequency. (ii) Intrinsic cellular noise was modeled using a fixed coefficient of variation of the jitter (i.e. independent of frequency), which corresponded to the noise level in FS cells firing at 30Hz. Data points are indicated by asterisks; linear fit of data is indicated by dashed line (slope=0.0007, $r=0.053$). The peak correlations were independent of frequency. This suggests that the increase in peak correlation with frequency is not due to interactions through electrical coupling, but rather is a result of an increased chance correlation due to the decrease in effective intrinsic noise with increased frequency.

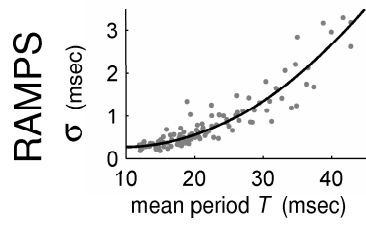
Supplementary Figure S8. Effects of heterogeneity on phase-locking. The frequency of one cell in an FS cell pair ($c_s = 0.31$) was ramped (red line) while the other received constant current in an attempt to maintain a fixed intrinsic frequency (black line). For large differences in intrinsic frequencies, cells can lock in non 1:1 phase-locked states. When the frequency of the cell being ramped was approximately twice that of the other, this relatively strongly coupled FS cell pair locked in a 2:1 phase locked state. This happened twice in this example due to an increase in frequency in the cell receiving the constant current injection, which was caused by current from the other cell.

Supplementary Figure S9. Effects of the strength of the “slow” potassium conductances g_{Kv1} at a fixed frequency of 25 Hz. blue lines: default g_{Kv1} ; green lines: default g_{Kv1} divided by 2; red lines: $g_{Kv1}=0$. **(A)** Changing g_{Kv1} leaves membrane voltage trace $V_o(t)$ almost unaltered. **(B)** PRCs $Z(t)$ for the different levels of g_{Kv1} . **(C,D)** G-functions for the different levels of g_{Kv1} . Decreasing g_{Kv1} leads to the destabilization of the anti-phase state. This shows that PRC shape can have major effects on the phase-locked states.

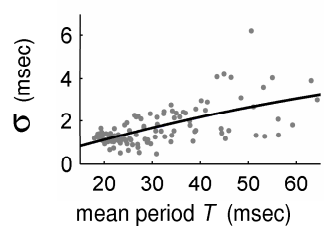
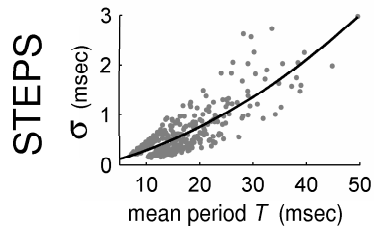
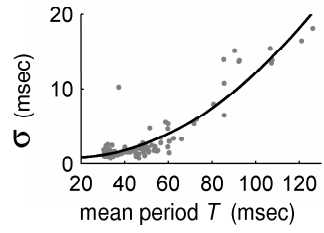
Supplementary Figure S10. Effects of the strength of the “fast high-threshold” potassium conductances g_{Kv3} at a fixed frequency of 25 Hz. blue lines: default g_{Kv1} ; green lines: default g_{Kv3} divided by 64. **(A)** Decreasing g_{Kv3} increases spike width and decreases AHP. **(B)** PRCs $Z(t)$ for the different levels of g_{Kv3} . **(C)** G-functions for the different levels of g_{Kv3} . Decreasing g_{Kv3} leads to the destabilization of the anti-phase state.

Supplementary Figure S11. Critical frequency for the stability of anti-phase *vs.* strength of potassium conductances g_{Kv1} and g_{Kv3} . Critical frequency increases with increases in the potassium conductances, i.e. these conductances promote stable anti-phase activity in FS model cell-pairs.

FS CELLS

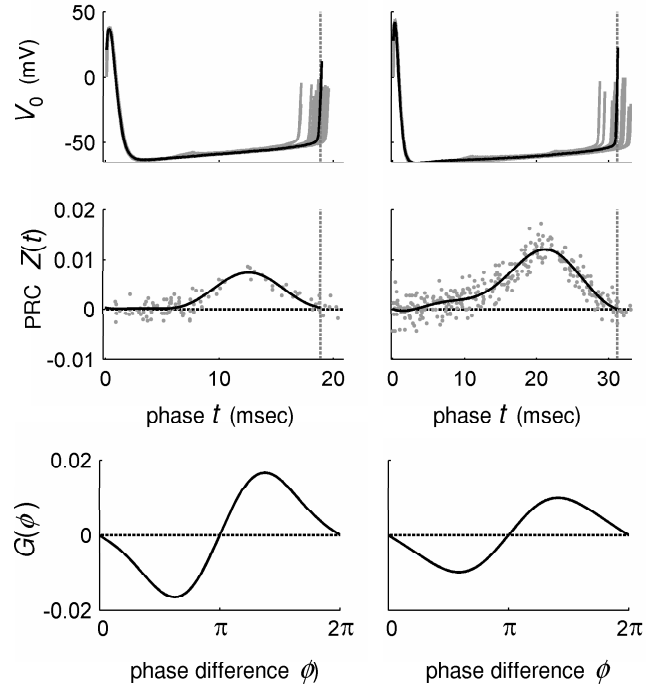


LTS CELLS

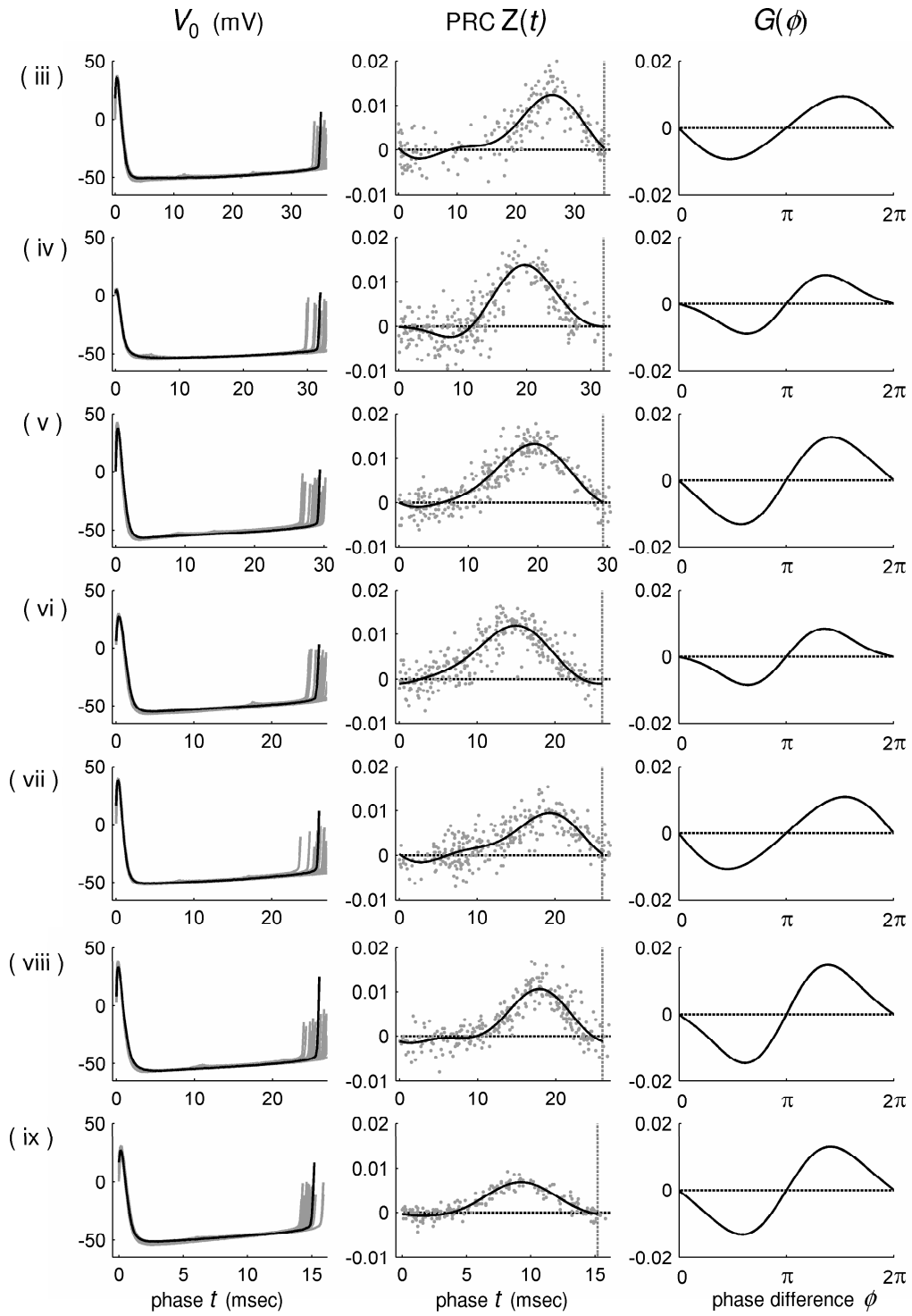


A 53 Hz

B 32 Hz



FS CELLS



LTS CELLS

